### Adjoint ferromagnets

Joaquín López-Suárez 1, Alexios P. Polychronakos2, Konstantinos Sfetsos1

<sup>1</sup>Department of Nuclear and Particle Physics, Faculty of Physics, National and Kapodistrian University of Athens, Athens 15784, Greece

jlopezs@phys.uoa.gr, ksfetsos@phys.uoa.gr

<sup>2</sup>Physics Department, the City College of New York, NY 10031, USA
The Graduate Center of the CUNY, New York, NY 10016, USA
apolychronakos@ccny.cuny.edu; apolychronakos@gc.cuny.edu

Wednesday 15<sup>th</sup> October, 2025

#### **Abstract**

We derive the phase structure and thermodynamics of ferromagnets consisting of elementary magnets carrying the adjoint representation of SU(N) and coupled through two-body quadratic interactions. Such systems have a continuous SU(N) symmetry as well as a discrete conjugation symmetry. We uncover a rich spectrum of phases and transitions, involving a paramagnetic and two distinct ferromagnetic phases that can coexist as stable and metastable states in different combinations over a range of temperatures. The ferromagnetic phases break SU(N) invariance in various channels, leading to spontaneous magnetization. Interestingly, the conjugation symmetry also breaks over a range of temperatures and group ranks N, providing a realization of a spontaneously broken discrete symmetry.

# Contents

1	Intr	oductio	n	2
2	The	e model	and the thermodynamic limit	3
	2.1	Equili	orium equations	5
	2.2	Stabili	ty	6
3	The	e adjoin	t representation	6
	3.1	Condi	tions for stability	10
		3.1.1	Stable solutions	10
4	Deta	ailed ar	alysis of the stable solutions	13
	4.1	Solutio	ons of type A	13
	4.2	Solutio	ons of type B	14
	4.3	Phases	s and transitions	15
		4.3.1	The $SU(2)$ case	16
		4.3.2	The $SU(3)$ case	16
		4.3.3	The $SU(4)$ and $SU(5)$ cases	16
		4.3.4	The $SU(6)$ case	18
		4.3.5	The $SU(7)$ case	19
		4.3.6	The $SU(8)$ case	19
		4.3.7	The cases $SU(N)$ with $N = 9, 10, 11 \dots \dots \dots \dots$	20
		4.3.8	The $SU(12)$ case	20
		4.3.9	The $SU(N)$ case with $N \geqslant 13$	20
		4.3.10	$SU(N)$ in the $N\gg 1$ limit	21
	4.4	The re	ducible fundamental-antifundamental representation	23
5	Con	clusion	ıs	23
A	On	conjuga	ate representations	25

#### C Some group theory results

28

### 1 Introduction

Magnetism with SU(N) degrees of freedom has been of increasing relevance, both in theoretical and experimental settings. Magnetic systems with SU(N) symmetry have been considered in the context of ultracold atoms [1–7], spin chains [8,9], interacting atoms on lattice cites [10–16], and were also studied in the presence of external SU(N) magnetic fields [17–19].

The thermodynamics and phase transitions of SU(N) ferromagnets, in particular, have proven extremely rich. In our recent work [20–24] we studied ferromagnets with each elementary magnet ("atom") carrying SU(N) degrees of freedom and two- or higher-body interactions and uncovered an intricate and nontrivial phase structure with qualitatively new features compared to standard SU(2) ferromagnets, even in situations where the only relevant parameter is the rank N of the group. We established the existence of several critical temperatures (as opposed to the single Curie temperature for SU(2)), metastability regimes, hysteresis phenomena, and spontaneous breaking of the global SU(N) symmetry into various channels. We also uncovered zero-temperature (quantum) phase transitions in the presence of three-body interactions. New critical phenomena emerge as the rank of the group becomes large, with a triple critical point appearing in an appropriate scaling limit.

The SU(N) representation carried by each atom is a defining element of the ferromagnet. The fundamental N-dimensional representation corresponds to the N internal states fully mixing under the action of the symmetry group. Higher representations correspond to reduced symmetry, in which interactions are still SU(N)-invariant, but the atom states are not arbitrarily mixed under the action of the symmetry group. In [23] we developed the formalism for dealing with a general atom representation  $\chi$ , and studied in detail the cases of the symmetric and antisymmetric irreducible representations (irreps), revealing the existence of additional phases and spontaneous symmetry breaking patterns.

In this paper we perform the analysis of the ferromagnet with atoms in the adjoint

representation by using the general formalism of [23]. This is a particularly interesting case. The adjoint irrep is self-conjugate, and consequently the ferromagnet has an additional discrete conjugation invariance symmetry. In this situation, one would expect a lower propensity to spontaneous SU(N) symmetry breaking, as most breaking channels have a preferred magnetization and would break the conjugation symmetry. Nevertheless, our analysis reveals that symmetry breaking phases with nontrivial magnetization do arise, all of them breaking SU(N) down to smaller subgroups, and some of them also breaking conjugation invariance. The phase structure is, if anything, richer than the one for the previously studied atom irreps and depends nontrivially on the rank N, with various critical temperatures emerging and rearranging as N increases, presenting a large set of phase transition scenaria. To probe the sensitivity of the model to relatively minor variants of its dynamics, we also study the case of the reducible fundamental-antifundamental atom representation (differing from the adjoint by the presence of an additional singlet state) and show that its phase structure is qualitatively similar to the one of the adjoint.

The organization of the paper is as follows: In section 2 we review the model of atoms with a general atom representation  $\chi$ , lay out the essential group theory facts required for its analysis, and derive its thermodynamic equilibrium and stability conditions. In section 3 we specialize to the case of the adjoint atom irrep, study its thermodynamics and stability conditions, and determine the structure of its possible stable phases. In section 4 we perform the analysis of the stable phases for various values of the group rank N, derive their critical temperatures, and determine their symmetry breaking patterns and cascade of phase transitions. We also perform the analysis of the reducible fundamental-atifundamental representation and compare the results to those for the adjoint. Finally, in section 5 we present our conclusions. A detailed analysis of unstable solutions and some group theory results are given in the appendices.

### 2 The model and the thermodynamic limit

We consider  $n \gg 1$  atoms at fixed positions, each carrying an irrep  $\chi$  of SU(N) and interacting with ferromagnetic two-body interactions. The analysis of [20,23] shows that, in the mean field approach, the ferromagnet can be described in terms of an effective coupling c and states transforming as irreps of the global SU(N) symmetry of the system, and we refer the reader to these papers for the details of the derivation.

The relevant mathematical quantities are the number of times each irrep of the global SU(N) is contained in the Hilbert space and the quadratic Casimirs of these irreps.

Irreps of SU(N) can be represented in terms of decreasing nonnegative integers  $k_i$ ,  $i=1,2,\ldots,N$ , related to Young tableau (YT) row lengths as  $\ell_i=k_i-k_N+i-N$  [25]. The multiplicity of irreps  $d_{n,\mathbf{k}}$  in the decomposition of the direct product of n representations  $\chi$  of SU(N) with character  $\chi(\mathbf{z})$  is given by

$$\sum_{\mathbf{k}} d_{n;\mathbf{k}} z_1^{k_1} \dots z_N^{k_N} = \Delta(\mathbf{z}) \chi^n(\mathbf{z}) , \qquad (2.1)$$

with  $z_i$  auxiliary variables corresponding to the eigenvalues of the fundamental group element  $U = \text{diag}\{\mathbf{z}\}$  (boldface  $\mathbf{k}$  stands for the collection  $\{k_i\}$  and similarly for  $\mathbf{z}$ ) and  $\Delta(\mathbf{z})$  being the Vandermonde determinant. Then  $d_{n;\mathbf{k}}$  obtains from a multiple integration in the complex  $\mathbf{z}$ -plane around the origin as

$$d_{n;\mathbf{k}} = \frac{1}{(2\pi i)^N} \prod_{i=1}^N \oint_C \frac{dz_i}{z_i^{k_i+1}} \Delta(\mathbf{z}) \chi^n(\mathbf{z}) .$$
 (2.2)

The partition function of the ferromagnet with atoms carrying the representation  $\chi$ , in the presence of magnetic fields  $B_i$  along the Cartan subalgebra of SU(N), is given by

$$Z = \sum_{\text{states}} e^{-\beta H} = \sum_{\langle \mathbf{k} \rangle} d_{n;\mathbf{k}} e^{\frac{\beta c}{n} C^{(2)}(\mathbf{k})} \operatorname{Tr}_{\mathbf{k}} \exp\left(\beta \sum_{j=1}^{N} B_{j} H_{j}\right), \qquad (2.3)$$

<**k**> representing non-negative decreasing integers and  $C^{(2)}(\mathbf{k})$  the quadratic Casimir of the irrep **k**. We are interested in the thermodynamic limit in which  $n \gg 1$ . Setting

$$k_i = nx_i \tag{2.4}$$

the  $x_i$  are of order 1 in the  $n \gg 1$  limit and constitute the magnetization parameters of the ferromagnet [20]. Keeping only leading orders in n, we obtain [23]

$$Z = \frac{n^N}{(2\pi i)^N} \prod_{i=1}^N \int dx_i \oint \frac{dz_i}{z_i} e^{-n\beta F(\mathbf{x}, \mathbf{z})} , \qquad (2.5)$$

where

$$F(\mathbf{x}, \mathbf{z}) = \sum_{i=1}^{N} \left( Tx_i \ln z_i - \frac{cx_i^2}{2} - B_i x_i \right) - T \ln \chi(\mathbf{z}) , \qquad (2.6)$$

is the free energy per atom.

### 2.1 Equilibrium equations

For  $n \gg 1$ , the integral in (2.5) is dominated by the saddle point of  $F(\mathbf{x}, \mathbf{z})$ . In the saddle-point approximation,  $F(\mathbf{x}, \mathbf{z})$  has to be stationary both in  $z_i$  and  $x_i$ , leading to the equilibrium conditions

$$\frac{\partial F}{\partial z_i} = T \left( \frac{x_i}{z_i} - \frac{\partial_{z_i} \chi}{\chi} \right) = 0,$$

$$\frac{\partial F}{\partial x_i} = T \ln z_i - cx_i - B_i = 0.$$
(2.7)

Note that even though the  $z_i$  are in principle complex, reality of  $x_i$  implies that the equilibrium  $z_i$  are real and positive. Hence, we define new variables  $w_i$  and  $\lambda$  as

$$z_i = e^{w_i} \,, \qquad \lambda = \ln \chi \,, \tag{2.8}$$

in terms of which the equilibrium equations for  $\mathbf{w}$  and  $\mathbf{x}$  become

$$x_i = \frac{\partial \lambda}{\partial w_i}$$
,  $Tw_i = cx_i + B_i$ . (2.9)

The free energy (2.6) is a function of both sets of variables  $x_i$  and  $w_i$ . Enforcing the equilibrium equation for  $w_i$  gives the specific free energy in terms of the magnetization parameters  $x_i$ ,

$$F(\mathbf{x}) = \sum_{i=1}^{N} \left( Tx_i w_i(\mathbf{x}) - \frac{c}{2} x_i^2 - B_i x_i \right) - T\lambda(\mathbf{w}(\mathbf{x})), \qquad (2.10)$$

 $w_i(\mathbf{x})$  being the solution of the first equation in (2.9). This expression is useful for the stability analysis around equilibrium configurations, as it is valid for arbitrary values of  $x_i$ . Enforcing also the equilibrium equation for  $x_i$ , the expression for  $F(\mathbf{x})$  simplifies to

$$F(\mathbf{x}) = \sum_{i=1}^{N} \frac{c}{2} x_i^2 - T\lambda \left( c\mathbf{x}/T + \mathbf{B}/T \right). \tag{2.11}$$

In fact, the above expression, taken off equilibrium, correctly reproduces both the equilibrium and the stability conditions for the system derived below.

For an irreducible representation, the character  $\chi$  is a homogeneous polynomial in the  $z_i$  with degree of homogeneity  $n_{\chi}$  the number of boxes in the YT of the irrep  $\chi$ . Summing the first of (2.9) over i, the right hand side gives the degree of homogeneity

of  $\chi$  and we obtain

$$\sum_{i=1}^{N} x_i = \sum_{i=1}^{N} \frac{\partial \lambda}{\partial w_i} = n_{\chi} . \tag{2.12}$$

This is a *constraint* on the variables  $x_i$ , necessary for (2.9) to have a solution for the  $w_i$ . If it is satisfied, the  $w_i$  are only determined up to a common additive constant.

We further note that the character  $\chi(\mathbf{z})$  is defined up to the transformation

$$\chi(\mathbf{z}) \to (z_1 \cdots z_N)^m \chi(\mathbf{z}), \qquad m \in \mathbb{Z},$$
 (2.13)

which changes the U(1) charge but preserves the SU(N) part of the irrep. From (2.9), the equilibrium  $x_i$  change as  $x_i \to x_i + m$  under this transformation, yielding the same irrep for the state, and the free energy (2.11) changes by a trivial constant.

### 2.2 Stability

We are interested in solutions of the equilibrium equations that are perturbatively stable. The analysis of [23] led to the stability criterion that the following two matrices should be positive semi-definite:

$$\Lambda \geqslant 0$$
,  $T \mathbb{1} - c\Lambda \geqslant 0$ , (2.14)

with

$$\Lambda_{ij} = \left. \frac{\partial^2 \lambda}{\partial w_i \partial w_j} \right|_{\mathbf{w} = (c\mathbf{x} + \mathbf{B})/T} = \left. \frac{1}{\chi} \frac{\partial^2 \chi}{\partial w_i \partial w_j} \right|_{\mathbf{w} = (c\mathbf{x} + \mathbf{B})/T} - x_i x_j.$$
 (2.15)

The subscript indicates that after the derivatives are taken we use the equilibrium equations.

## 3 The adjoint representation

We focus on the ferromagnet with atoms in the adjoint representation in the absence of external fields. In what follows, we set the magnetic fields  $B_i$  to zero.

The YT for the adjoint representation is conveniently presented by using the notation

$$s \text{ antiboxes} \left\{ \begin{array}{c} \bullet \\ \vdots \\ \bullet \end{array} \right\} N - s \text{ boxes}. \tag{3.1}$$

Then, the YT for the adjoint representation is

$$= :$$

$$N \text{ boxes}.$$

$$(3.2)$$

The character in terms of the variables  $z_i$  is [25]

$$\chi(\mathbf{z}) = \left(\sum_{i=1}^{N} z_i\right) \left(\sum_{i=1}^{N} z_i^{-1}\right) - 1.$$
(3.3)

This corresponds to the box-antibox representation, in which the total number of boxes is  $n_{\text{adj}} = 0$  (in the representation in terms of boxes we would have  $n_{\text{adj}} = N$ ). Consequently, the constraint (2.12) becomes

$$\sum_{i=1}^{N} x_i = 0. {(3.4)}$$

In the box-antibox representation, we can directly interpret  $nx_i$  as the number of boxes (for  $x_i > 0$ ) or antiboxes (for  $x_i < 0$ ) in row i of the YT of the configuration  $\mathbf{x}$ . (The box-only representation corresponds to row lengths  $\ell_i = n(x_i - x_N)$  to leading order in n.) The free energy is invariant under the transformation  $x_i \to -x_i$ , which corresponds to turning the irrep parametrized by  $x_i$  to its conjugate. This conjugation invariance is a corollary of the fact that the adjoint irrep of the atoms is self-conjugate.

To efficiently analyze the equilibrium conditions, we define new variables

$$\alpha_i = w_i + \mu$$
,  $\mu = \frac{1}{2} \ln \frac{\sum_{j=1}^N z_j^{-1}}{\sum_{j=1}^N z_j}$ , (3.5)

( $\mu$  absorbs the arbitrary constant in the definition of  $w_i$ ). The  $\alpha_i$  are subject to the constraints

$$\sum_{i=1}^{N} e^{\alpha_i} = \sum_{i=1}^{N} e^{-\alpha_i} = \rho , \quad \rho^2 \equiv \sum_{i,j=1}^{N} z_i z_j^{-1} = \chi(\mathbf{z}) + \mathbf{1} . \tag{3.6}$$

Clearly  $\rho \geqslant N$ . Then, the first of (2.9) gives

$$x_i = \frac{2\rho}{\rho^2 - 1} \sinh \alpha_i$$
,  $i = 1, 2, ..., N$ , (3.7)

which, due to the constraints (3.6), implies (3.4), in agreement with (2.12). The second equation in (2.9) becomes

$$\alpha_i - \frac{T_0(\rho)}{T} \sinh \alpha_i = \mu, \qquad i = 1, 2, \dots, N,$$
(3.8)

where

$$T_0(\rho) = \frac{2\rho}{\rho^2 - 1} c$$
,  $0 < T_0(\rho) < T_0(N) = \frac{2N}{N^2 - 1} c \equiv T_0$ . (3.9)

 $T_0$  denotes the maximal value of  $T_0(\rho)$ , in terms of which c is expressed as

$$c = \frac{N^2 - 1}{2N} T_0. (3.10)$$

Similarly to previous work [20,23],  $T_0$  will turn out to be the temperature below which the singlet becomes unstable. It is interesting that c can be written in the general group theoretical form (C.1) which also applies to the fundamental, symmetric, and antisymmetric atom representations studied in [23].

Equations (3.8) and the two constraints (3.6) determine the  $\alpha_i$  and the two Lagrange multiplier-like variables  $\rho$  and  $\mu$ . For fixed  $\rho$  and  $\mu$ , all  $\alpha_i$  obey the same equation. This equation can have either one or three solutions, depending on whether the ratio  $T_0(\rho)/T$  is larger or smaller than unity (see fig. 1). However, the single solution

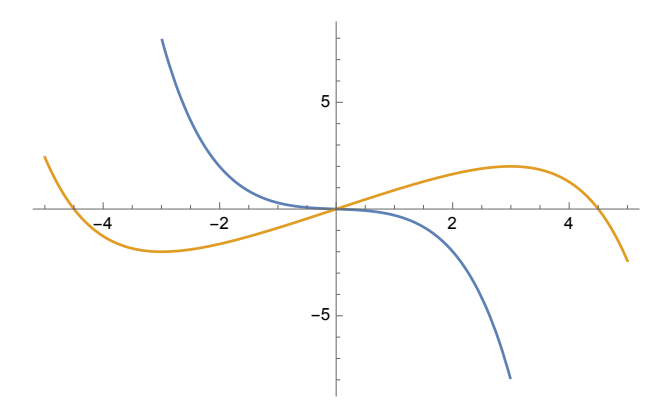


Figure 1: Plots of the left hand side of (3.8) for  $T < T_0(\rho)$  (blue) and for  $T > T_0(\rho)$  (yellow).

case is acceptable only for  $\alpha_i = 0$  (corresponding to  $x_i = 0$ ,  $\rho = N$ ) since otherwise the constraint (3.4) cannot be satisfied. This corresponds to the singlet state with no spontaneous magnetization.

In the three solution case, not all of the  $\alpha_i$  can have the same sign, otherwise the constraint (3.4) cannot be satisfied. Since the state is invariant under permutations of the  $\alpha_i$ , we may choose the ordering of the solutions

$$\alpha_3 < \alpha_2 < \alpha_1$$
,  $\alpha_3 < 0$ ,  $\alpha_1 > 0$ . (3.11)

We will denote by  $p_1$  the number of  $\alpha_i$  corresponding to the solution  $\alpha_1$  and similarly for the solutions  $\alpha_2$  and  $\alpha_3$ . The  $p_i$  clearly obey

$$p_1 + p_2 + p_3 = N$$
,  $p_{1,2,3} = 0, 1, ..., N - 1$ . (3.12)

Note that this condition for N=2 has as only solution (without loss of generality)  $p_1=p_3=1, p_2=0$ . The case of SU(2) will be treated separately.

From here on, we focus to  $N \ge 3$ . Then the constraint (3.4) becomes

$$p_1 \sinh \alpha_1 + p_2 \sinh \alpha_2 + p_3 \sinh \alpha_3 = 0$$
. (3.13)

Finally, (3.6) implies

$$\rho = p_1 e^{\alpha_1} + p_2 e^{\alpha_2} + p_3 e^{\alpha_3} = p_1 e^{-\alpha_1} + p_2 e^{-\alpha_2} + p_3 e^{-\alpha_3}. \tag{3.14}$$

This solution corresponds to a YT with  $p_1 + p_2$  rows, the first  $p_1$  of them of equal length  $\ell_1 = (x_1 - x_3)n$  and the remaining  $p_2$  of equal length  $\ell_2 = (x_1 - x_3)n$ . That is,

To solve the equations and determine  $\alpha_{1,2,3}$ , we first choose  $p_i$  obeying (3.12). Then, assuming  $p_3 \neq 0$ , we may use (3.13) to solve for  $\alpha_3$  in terms of  $\alpha_1$  and  $\alpha_2$ 

$$\alpha_3 = -\ln\left(f + \sqrt{f^2 + 1}\right), \qquad f = \frac{p_1}{p_3}\sinh\alpha_1 + \frac{p_2}{p_3}\sinh\alpha_2$$
 (3.16)

and then determine the latter from the system of transcendental equations

$$\alpha_1 - \frac{T_0(\rho)}{T} \sinh \alpha_1 = \alpha_2 - \frac{T_0(\rho)}{T} \sinh \alpha_2 ,$$

$$\alpha_1 - \frac{T_0(\rho)}{T} \sinh \alpha_1 = \alpha_3 - \frac{T_0(\rho)}{T} \sinh \alpha_3 ,$$
(3.17)

where  $T_0(\rho)$  in (3.9) is found using (3.14). Hence, (3.17) is a system with two unknowns  $\alpha_1$  and  $\alpha_2$ , which can be chosen as in (3.11). The free energy at equilibrium is

$$F(T) = T_0 \frac{\rho^2 (N^2 - 1)}{N(\rho^2 - 1)^2} \sum_{i=1}^{N} \sinh^2 \alpha_i - T \ln(\rho^2 - 1)$$

$$= T_0 \frac{\rho^2 (N^2 - 1)}{N(\rho^2 - 1)^2} (p_1 \sinh^2 \alpha_1 + p_2 \sinh^2 \alpha_2 + p_3 \sinh^2 \alpha_3) - T \ln(\rho^2 - 1),$$
(3.18)

where we used the equilibrium equation (3.8) and the constraint (3.4) and where in the second line we specialized to the three solution case. For the singlet, the free energy is

$$F_{\text{singlet}}(T) = -T \ln(N^2 - 1)$$
 (3.19)

### 3.1 Conditions for stability

From (2.15), using (3.3) and (3.6), we obtain for the matrix  $\Lambda_{ij}$  the expression

$$\Lambda_{ij} = \frac{z_i \left(\sum_{j=1}^N z_j^{-1}\right) + z_i^{-1} \left(\sum_{j=1}^N z_j\right)}{\rho^2 - 1} \,\delta_{ij} - \frac{z_i z_j^{-1} + z_j z_i^{-1}}{\rho^2 - 1} - x_i x_j \,. \tag{3.20}$$

Further using (3.5) and (3.7), we obtain the final expression in terms of  $\alpha_i$ 

$$\Lambda_{ij} = \frac{2}{\rho^2 - 1} \left( \rho \cosh \alpha_i \delta_{ij} - \cosh \alpha_i \cosh \alpha_j - \frac{\rho^2 + 1}{\rho^2 - 1} \sinh \alpha_i \sinh \alpha_j \right). \tag{3.21}$$

This is of the form examined in [23] parametrized in terms of a Euclidean signature metric and two *N*-dimensional vectors.

#### 3.1.1 Stable solutions

The matrix  $\Lambda_{ij}$  has to satisfy the stability conditions (2.14). It turns out that the first of them,  $\Lambda \geqslant 0$ , is trivially satisfied, so we focus on the second one. For the generic solution corresponding to a YT of  $p_1$  rows of length  $\ell_1$  followed by  $p_2$  rows of length

 $\ell_2 < \ell_1$ , an exhaustive numerical investigation of the stability condition (2.14) reveals that such solutions are generically unstable, with the following exceptions:

A: 
$$\bigcirc$$
 or  $\bigcirc$  (3.22)

and

$$B: \quad \bullet \bullet \cdots \bullet \qquad , \qquad (3.23)$$

as well the singlet, which we will denote with a thick dot

Singlet: 
$$\bullet$$
 (3.24)

These states can be stable, metastable, or unstable depending on the temperature range. The two YT in the configuration A are of equal length, and the corresponding solutions are degenerate, having the same free energy. Configuration B has an equal number of boxes and antiboxes, so their YT has one row of length  $\ell_1$  and (N-2)-rows of length  $\ell_2 = \ell_1/2$ . The two configurations in A are related by conjugation, while B is self-conjugate. (Some elementary properties of the conjugate YT adopted to our context are included in the appendix A.)

Hence, solutions A represent a phase of spontaneously broken conjugation symmetry, while B a phase of unbroken conjugation symmetry. The corresponding SU(N) symmetry breaking patterns are

A: 
$$SU(N) \rightarrow SU(N-1) \times U(1)$$
,  
B:  $SU(N) \rightarrow SU(N-2) \times U(1) \times U(1)$ . (3.25)

We stress that there are solutions other than those of type A and type B, but they are unstable. For instance, solutions with  $p_1 = 2$  and  $p_2 = N - 4$  are self-conjugate but unstable. To illustrate this, we plotted the eigenvalues of the stability matrix  $T \mathbb{1} - c\Lambda$  in (2.14) as a function of the temperature for solutions of type A (fig. 2) and type B (fig. 3), for  $p_1 = 1$  and their extensions for  $p_1 = 2$ . We have also examined other non-self conjugate solutions, some of them given in appendix B, and they turn out to be unstable as well.

The fact that only configurations A and B with a single row and a single antirow are stable can qualitatively be traced to the fact that, when the atoms carry the fundamental representation, only one-row YTs are stable [20]. Similarly, if the atoms carry the

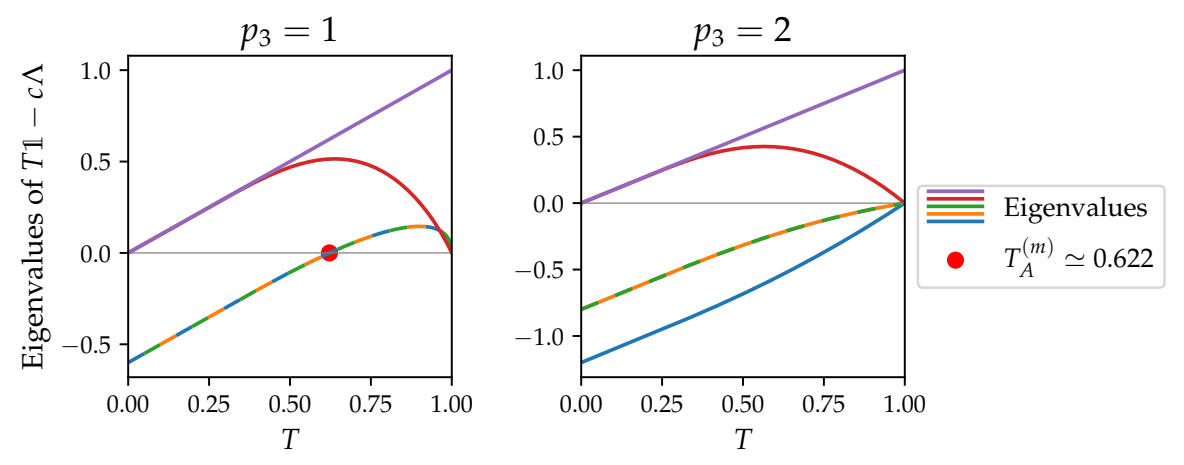


Figure 2: Eigenvalues of  $T\mathbb{1} - c\Lambda$  for a solution of type A and N = 5, for  $p_3 = 1$  (left) and  $p_3 = 2$  (right). In the former case, all eigenvalues are positive for temperatures  $T_A^{(m)} < T < 1$ , whereas in the latter one several eigenvalues are negative in the full temperature range in which the solutions exist. Temperatures are in units of  $T_0$ , and multi-colored lines represent degenerate eigenvalues.

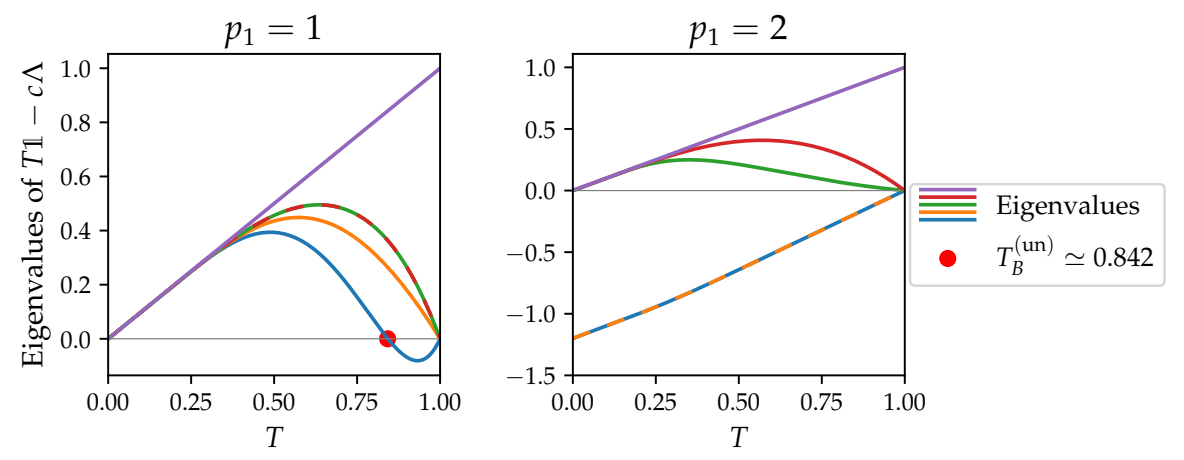


Figure 3: Eigenvalues of  $T\mathbb{1} - c\Lambda$  for a solution of type B and N = 5, for  $p_1 = 1$  (left) and  $p_1 = 2$  (right). Temperatures are in units of  $T_0$ . For  $p_1 = 1$ , the solution is stable for temperatures below  $T_{\rm B}^{({\rm un})}$ , whereas for  $p_1 = 2$  the solution is unstable for all temperatures. Multi-colored lines represent degenerate eigenvalues.

antifundamental representation, only the conjugate one-antirow YTs are stable. Since the adjoint can be thought of as a direct product of the fundamental and the antifundamental representations with the singlet removed (see section 4.4), A and B are solutions that incorporate the aforementioned one-row properties.

### 4 Detailed analysis of the stable solutions

### 4.1 Solutions of type A

First we examine the case in which the  $\alpha_i$  have only two distinct values. This corresponds to, say,  $p_2 = 0$ , with  $p_1$  of the  $\alpha_i$  at solution  $\alpha_1 > 0$  and  $p_3 = N - p_1$  at the solution  $\alpha_3 < 0$ . Then the constraint (3.13) gives for  $\alpha_3$ 

$$\alpha_3 = -\ln\left(f + \sqrt{f^2 + 1}\right), \qquad f = \frac{N - p_3}{p_3}\sinh\alpha_1$$
 (4.1)

and  $\alpha_1$  is determined from the transcendental equation

$$\alpha_1 - \alpha_3 - \frac{NT_0(\rho)}{p_3 T} \sinh \alpha_1 = 0, \qquad (4.2)$$

where  $T_0(\rho)$  is as in (3.9) with

$$\rho = (N - p_3)e^{\alpha_1} + p_3(-f + \sqrt{1 + f^2}). \tag{4.3}$$

The case  $p_1 = 1$  correspond to a single row, and the case  $p_3 = 1$  to a single antirow, as in states A. Focusing on the one-antirow stable solution in A with  $p_3 = 1$ , the left hand side of (4.2) is positive for  $\alpha_1 \gg 1$ , while an expansion in  $\alpha_1 \ll 1$  yields

$$\left(1 - \frac{T_0}{T}\right)\alpha_1 - \frac{(N^2 - 1)(N - 2)T - (3N^2 - N + 2)T_0}{6(N + 1)T}\alpha_1^3 + \mathcal{O}(\alpha_1)^5 = 0.$$
(4.4)

For  $T < T_0$  the first term starts out negative, and given the behavior for  $\alpha_1 \gg 1$ , a solution must exist for a finite value of  $\alpha_1$  as depicted in fig. 4.

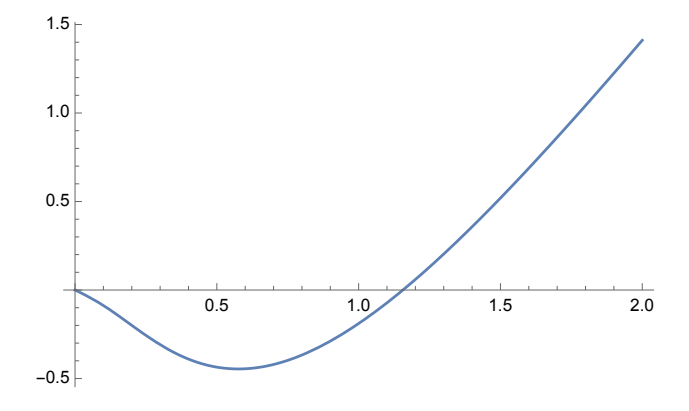


Figure 4: Plot of the left hand side of (4.2) for  $T < T_0$ .

For  $T > T_0$  the first term starts out positive. In order for a non-vanishing solution

to exist the coefficient of the cubic term needs to be negative (assuming that the first zero occurs for small  $\alpha_1$  which is the case for T slightly larger than  $T_0$ ). Setting  $T=T_0$  in this term, we see that it turns negative for N>5. Hence for small enough  $T>T_0$  and  $N\geqslant 6$ , (4.2) will have a nonzero solution. We may compute the critical temperature  $T_A^{(c)}$  below which this solution exists by simultaneously setting (4.9) and its first derivative with respect to  $\alpha_1$  to zero. That gives a system of two transcendental equations for  $T_A^{(c)}$  and  $\alpha_{1c}$  which has solutions only for  $N\geqslant 6$ . The various cases are depicted in fig. 5

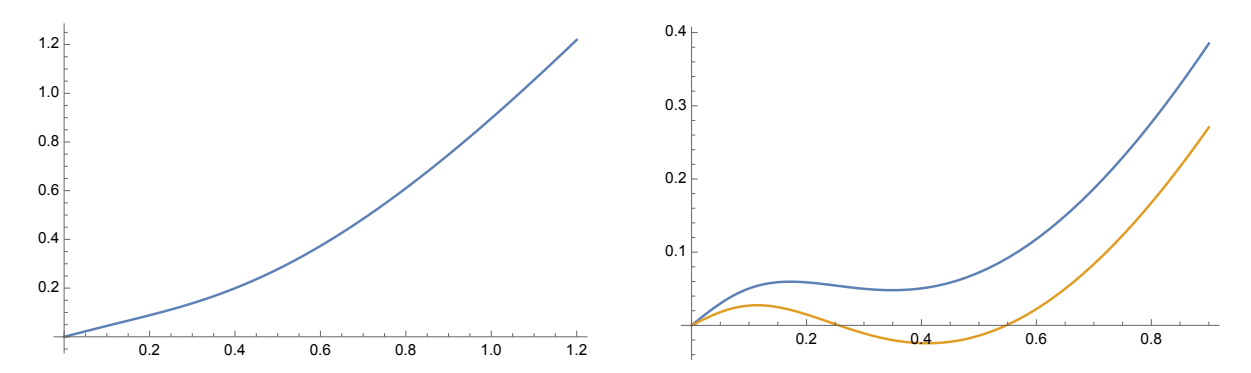


Figure 5: Left plot: the left hand side of (4.2) for  $T > T_0$ , for N = 3, 4, 5. Right plot: the left hand side of (4.2) for  $N \ge 6$  for  $T_0 < T_A^{(c)} < T$  (in blue) and for  $T_0 < T < T_A^{(c)}$  (in yellow).

The free energy (3.18) becomes (for general  $p_3$ )

$$F(T) = T_0 \frac{\rho^2 (N^2 - 1)(N - p_3)}{p_3(\rho^2 - 1)^2} \sinh^2 \alpha_1 - T \ln(\rho^2 - 1).$$
 (4.5)

### 4.2 Solutions of type B

Consider next the case where one of the three solutions of (3.8) is zero, say  $\alpha_2 = 0$ , which enforces  $\mu = 0$ . Then from (3.8) and (3.13) we have that  $p_1\alpha_1 + p_3\alpha_3 = 0$ . This and (3.13) imply

$$\sinh \frac{p_1}{p_3} \alpha_1 = \frac{p_1}{p_3} \sinh \alpha_1 , \qquad (4.6)$$

which, for  $\alpha_1 \neq 0$ , can only be satisfied if  $p_3 = p_1$ . This implies  $\alpha_3 = -\alpha_1$ , and (3.8) becomes

$$\alpha_1 - \frac{T_0(\rho)}{T} \sinh \alpha_1 = 0 , \qquad (4.7)$$

where  $T_0(\rho)$  is given by (3.9) with

$$\rho = N + 4p_1 \sinh^2 \frac{\alpha_1}{2} , \qquad T_0(\rho) = 2T_0 \frac{N + 4p_1 \sinh^2 \frac{\alpha_1}{2}}{(N + 4p_1 \sinh^2 \frac{\alpha_1}{2})^2 - 1} . \tag{4.8}$$

We eventually obtain the transcendental equation

$$\alpha_1 - \frac{N^2 - 1}{N} \frac{T_0}{T} \frac{N + 4p_1 \sinh^2 \frac{\alpha_1}{2}}{(N + 4p_1 \sinh^2 \frac{\alpha_1}{2})^2 - 1} \sinh \alpha_1 = 0.$$
 (4.9)

Focusing on the stable solution in B with  $p_1 = 1$ , the analysis proceeds as in case A. For  $\alpha_1 \gg 1$  the left hand side of (4.9) is positive, while an expansion in  $a_1 \ll 1$  yields

$$\left(1 - \frac{T_0}{T}\right)\alpha_1 - \frac{T_0}{T}\frac{N^3 - 6N^2 - N - 6}{6N(N^2 - 1)}\alpha_1^3 + \mathcal{O}(\alpha_1)^5 = 0.$$
 (4.10)

For  $T < T_0$  the first term starts out negative, and given the behavior for  $a_1 \gg 1$ , a solution must exist for a finite value of  $\alpha_1$ . For  $T > T_0$  the first term starts out positive. In order for a solution to exist the coefficient of the cubic term needs to be negative (assuming that the first zero occurs for small  $\alpha_1$  which is the case for T slightly larger than  $T_0$ ). We see that it turns negative for N > 6. Hence, for  $N \geqslant 7$  and for small enough  $T > T_0$ , (4.9) will have a nonzero solution. We may compute the critical temperature  $T_B^{(c)}$  below which this solution exists by simultaneously setting (4.9) and its first derivative with respect to  $\alpha_1$  to zero. That gives a system of two transcendental equations for  $T_A^{(c)}$  and  $\alpha_{1c}$  which has solutions only for  $N \geqslant 7$ . The plots of the left hand side of (4.9) are qualitatively similar to those in fig. 4 and fig. 5.

The free energy (3.18) becomes (for  $p_1 = 1$ )

$$F(T) = 2T_0 \frac{N^2 - 1}{N} \left( \frac{\left(N + 4\sinh^2\frac{\alpha_1}{2}\right)\sinh\alpha_1}{\left(N + 4\sinh^2\frac{\alpha_1}{2}\right)^2 - 1} \right)^2 - T \ln\left(\left(N + 4\sinh^2\frac{\alpha_1}{2}\right)^2 - 1\right). \quad (4.11)$$

#### 4.3 Phases and transitions

At low temperatures, the stable configuration is B for all values of N. Similarly, for high temperatures the singlet is the only solution and it is stable. For intermediate temperatures and  $N \geqslant 4$ , the conjugation symmetry breaking phase A also appears, and configurations can become stable, metastable, or cease to exist. For N=3, the situation is simple and presented in table 1. For  $N\geqslant 4$ , there are subtle differences depending on the values of N, and unexpectedly numerous cases appear, which we present below in detail. Focusing on the stable phases only, the presentation simplifies and is given in table 3 for N=4, 5 and in table 5 for  $N\geqslant 6$ .

#### **4.3.1** The SU(2) case

In [26] the decomposition of n spin-s irreps of SU(2) was presented and a ferromagnetic model similar to the one we consider here was studied in the mean field approximation. Since s=1 corresponds to the adjoint SU(2) irrep, the s=1 results should match those of the present paper. Indeed, letting s=1 in eq. (4.20) of [26] and also rescaling  $c \to 2c$  in order to match conventions, we obtain

$$\frac{2\sinh\tau}{2\cosh\tau+1} = \frac{\tau T}{2c} \,. \tag{4.12}$$

A non-vanishing solution for  $\tau$  implies a magnetized configuration. (4.12) becomes (4.9) upon setting N=2,  $c=3T_0/4$ ,  $p_1=1$  and defining  $\tau=2\alpha_1$ . The corresponding one-row YT derived in [26] also matches the one derived in the present paper.

#### **4.3.2** The SU(3) case

For SU(3) we have a simple picture, depicted in table 1. In this case, configuration A is never stable for  $T < T_0$ . We note that in this case the YT that corresponds to

irrep	$T < T_0$	$T_0 < T$
•	unstable	stable
В	stable	×
A	unstable	×

Table 1: Phases in various temperature ranges for N=3 and their stability characterization.

configuration B is simply

B for 
$$SU(3)$$
:  $(4.13)$ 

#### **4.3.3** The SU(4) and SU(5) cases

The situation is more complicated, with several critical temperatures listed from low to high: a temperature  $T_A^{(m)}$  at which the configuration A becomes from unstable metastable; a higher temperate  $T_{BA}$  at which configurations B and A exchange their metastability; and an even higher temperature  $T_B^{(un)}$  at which configuration B becomes unstable. All these temperatures are smaller than  $T_0$ , above which only the singlet exists and is stable. We have tabulated the results in table 2.

Temperature/irrep	В	A	•
$T < T_{ m A}^{( m m)}$	stable	unstable	unstable
$T_{\rm A}^{\rm (m)} < T < T_{\rm BA}$	stable	metastable	unstable
$T_{\rm BA} < T < T_{\rm B}^{\rm (un)}$	metastable	stable	unstable
$T_{\rm B}^{\rm (un)} < T < T_0$	unstable	stable	unstable
$T_0 < T$	×	×	stable

Table 2: Phases in various temperature ranges for N = 4,5 and their stability.

Table 3 depicts only the stable configurations in each temperature range.

Temperature	$T < T_{\rm BA}$	$T_{\rm BA} < T < T_0$	$T_0 < T$
irrep	В	A	•

Table 3: Stable phases in the various temperature ranges for N = 4, 5.

For all cases up to N=5 there is a phase transition at  $T=T_0$ . We may compute the order of the phase transition by examining the free energy of the solutions at this transition temperature. For the cases with N=4,5 we have a transition from the solution A to the singlet so that we may use for the free energy that in (4.5) for  $p_3=1$ . For N=3 we may use the free energy in (4.11) for the B solution. For N=2 either (4.5) or (4.11) since the A and B solutions coincide. For  $T\lesssim T_0$  we have the expansions

$$\alpha_1 = c_1 \sqrt{T_0 - T} \left( 1 + c_2 (T_0 - T) + \dots \right),$$

$$N = 2: \quad c_1 = \sqrt{\frac{3}{2}}, \quad c_2 = \frac{13}{20},$$

$$N = 3: \quad c_1 = 2, \quad c_2 = \frac{11}{15},$$

$$N = 4: \quad c_1 = \frac{1}{2} \sqrt{\frac{15}{2}}, \quad c_2 = \frac{9}{8},$$
(4.14)

where we have used the either the equation for the A solution or the B solution (for N=3). This gives the expansion of the free energy for  $T \lesssim T_0$  which compactly takes the form

$$F(T) = -T \ln(N^2 - 1) + \frac{3}{N - 5} (T - T_0)^2 + \dots, \quad N = 2, 3, 4.$$
 (4.15)

For  $T > T_0$ , the free energy of the singlet is  $-T \ln(N^2 - 1)$ . Hence,  $T_0$  marks a second order phase transition.

For N = 5 things are a bit different. We find that

$$\alpha_1 = \frac{\sqrt{6}}{5^{3/4}} (T_0 - T)^{1/4} \left( 1 + \frac{461}{140\sqrt{5}} (T_0 - T)^{1/2} + \dots \right). \tag{4.16}$$

Then the expansion of the free energy for  $T \lesssim T_0$  is

$$F(T) = -T \ln 24 - \frac{2\sqrt{5}}{3} (T_0 - T)^{3/2} + \dots, \quad N = 5.$$
 (4.17)

Hence, the transition can be characterized as a second order one, albeit the second derivative becomes infinite.

The metastability transition at  $T_{BA}$  is first order, as is generically the case.

#### **4.3.4** The SU(6) case

In this case, configuration A exists for temperatures above  $T_0$  up to a temperature  $T_{\rm A}^{(c)}$ , and there is a temperature  $T_{\rm AS}$  such that  $T_0 < T_{\rm AS} < T_{\rm A}^{(c)}$  at which A and the singlet exchange metastabilty roles. The results are presented in table 4.

Temperature/irrep	В	A	•
$T < T_{\rm A}^{(\rm m)}$	stable	unstable	unstable
$T_{\rm A}^{\rm (m)} < T < T_{\rm BA}$	stable	metastable	unstable
$T_{\rm BA} < T < T_{\rm B}^{\rm (un)}$	metastable	stable	unstable
$T_{\rm B}^{\rm (un)} < T < T_0$	unstable	stable	unstable
$T_0 < T < T_{AS}$	×	stable	metastable
$T_{\mathrm{AS}} < T < T_{\mathrm{A}}^{(c)}$	×	metastable	stable
$T_{ m A}^{(c)} < T$	×	×	stable

Table 4: Phases in various temperature ranges for N = 6 and their stability.

The phase transition between the B and the A solutions at  $T_{BA}$  is first order similar to the cases with  $N \le 5$ . However, unlike these cases, for N = 6 the phase transition between the A solution and the singlet is first order, instead of second, and is happening at  $T_{AS} > T_0$ . This feature persists for all higher values of N.

We may construct the smaller table 5 with only the stable configurations in each temperature range. In fact this covers all cases with  $N \ge 6$  and will not be repeated subsequently.

This is similar to table 3, the only difference being that the singlet takes over at the

Temperature	$T < T_{\rm BA}$	$T_{\rm BA} < T < T_{\rm AS}$	$T_{\rm AS} < T$
irrep	В	A	•

Table 5: Stable phases in the various temperature ranges for  $N \ge 6$ .

temperature  $T_{AS} > T_0$ . So the result of tables 5 and 3 is that for high temperatures the SU(N) symmetry as well as the conjugation symmetry are intact, for intermediate temperatures both are broken, whereas for low enough temperatures conjugation is restored. The breaking patterns are given in (3.25).

### **4.3.5** The SU(7) case

In this case the configuration B also exists above  $T_0$  up to a temperature  $T_{\rm B}^{(c)}$ , with  $T_0 < T_{\rm B}^{(c)} < T_{\rm AS}$ . The results are presented in table 6.

Temperature/irrep	В	A	•
$T < T_{ m A}^{( m m)}$	stable	unstable	unstable
$T_{\rm A}^{\rm (m)} < T < T_{\rm BA}$	stable	metastable	unstable
$T_{\rm BA} < T < T_{\rm B}^{\rm (un)}$	metastable	stable	unstable
$T_{\rm B}^{\rm (un)} < T < T_0$	unstable	stable	unstable
$T_0 < T < T_{\rm B}^{(c)}$	unstable	stable	metastable
$T_{\rm B}^{(c)} < T < T_{\rm AS}$	×	stable	metastable
$T_{\mathrm{AS}} < T < T_{\mathrm{A}}^{(c)}$	×	metastable	stable
$T_{ m A}^{(c)} < T$	×	×	stable

Table 6: Phases in various temperature ranges for N = 7 and their stability.

Note the ordering of temperatures  $T_{BA} < T_{B}^{(un)} < T_{0}$ . This ordering will change with higher values of N.

In general, for  $N \ge 6$  the eigenvalues of the stability matrix  $T \mathbb{1} - c\Lambda$  as a function of the temperature have similar plots to those in fig. 2 and fig. 3, with the difference that they extend to temperatures higher than  $T_0$ , and will not be presented here.

#### **4.3.6** The SU(8) case

As noted, the ordering of the various critical temperatures changes as N increases, until it stabilizes for  $N \geqslant 13$ . In the case of N=8 the ordering of temperatures changes to  $T_{\rm BA} < T_0 < T_{\rm B}^{\rm (un)}$ . The results are presented in table 7.

Temperature/irrep	В	A	•
$T < T_{ m A}^{( m m)}$	stable	unstable	unstable
$T_{\rm A}^{\rm (m)} < T < T_{\rm BA}$	stable	metastable	unstable
$T_{\rm BA} < T < T_0$	metastable	stable	unstable
$T_0 < T < T_{\rm B}^{\rm (un)}$	metastable	stable	metastable
$T_{\rm B}^{\rm (un)} < T < T_{\rm B}^{(c)}$	unstable	stable	metastable
$T_{\rm B}^{(c)} < T < T_{\rm AS}$	×	stable	metastable
$T_{\rm AS} < T < T_{\rm A}^{(c)}$	×	metastable	stable
$T_{\rm A}^{(c)} < T$	×	×	stable

Table 7: Phases in various temperature ranges for N=8 and their stability.

#### **4.3.7** The cases SU(N) with N = 9, 10, 11

In this case the ordering of temperatures changes to  $T_0 < T_{BA} < T_B^{(un)}$ . The results are presented in table 8.

Temperature/irrep	В	A	•
$T < T_{ m A}^{( m m)}$	stable	unstable	unstable
$T_{\rm A}^{\rm (m)} < T < T_0$	stable	metastable	unstable
$T_0 < T < T_{\mathrm{BA}}$	stable	metastable	metastable
$T_{\rm BA} < T < T_{\rm B}^{\rm (un)}$	metastable	stable	metastable
$T_{\rm B}^{\rm (un)} < T < T_{\rm B}^{(c)}$	unstable	stable	metastable
$T_{\rm B}^{(c)} < T < T_{\rm AS}$	×	stable	metastable
$T_{\rm AS} < T < T_{\rm A}^{(c)}$	×	metastable	stable
$T_{\rm A}^{(c)} < T$	×	×	stable

Table 8: Phases in various temperature ranges for N = 9, 10, 11 and their stability.

Note the ordering of temperatures  $T_{\rm B}^{(c)} < T_{\rm AS}$  which will change subsequently.

#### **4.3.8** The SU(12) case

In this case the ordering changes to  $T_{AS} < T_{B}^{(c)}$ . The results are presented in table 9.

### **4.3.9** The SU(N) case with $N \ge 13$

In this case the ordering changes to  $T_{\rm AS} < T_{\rm B}^{({\rm un})}$ . The results are presented in table 10.

Temperature/irrep	В	A	•
$T < T_{ m A}^{( m m)}$	stable	unstable	unstable
$T_{A}^{(m)} < T < T_0$	stable	metastable	unstable
$T_0 < T < T_{\mathrm{BA}}$	stable	metastable	metastable
$T_{\rm BA} < T < T_{\rm B}^{\rm (un)}$	metastable	stable	metastable
$T_{\rm B}^{\rm (un)} < T < T_{\rm AS}$	unstable	stable	metastable
$T_{\rm AS} < T < T_{\rm B}^{(c)}$	unstable	metastable	stable
$T_{\rm B}^{(c)} < T < T_{\rm A}^{(c)}$	×	metastable	stable
$T_{\rm A}^{(c)} < T$	×	×	stable

Table 9: Phases in various temperature ranges for N = 12 and their stability.

Temperature/irrep	В	A	•
$T < T_{ m A}^{( m m)}$	stable	unstable	unstable
$T_{\rm A}^{\rm (m)} < T < T_0$	stable	metastable	unstable
$T_0 < T < T_{\mathrm{BA}}$	stable	metastable	metastable
$T_{\rm BA} < T < T_{\rm AS}$	metastable	stable	metastable
$T_{\rm AS} < T < T_{\rm B}^{\rm (un)}$	metastable	metastable	stable
$T_{\rm B}^{\rm (un)} < T < T_{\rm B}^{\rm (c)}$	unstable	metastable	stable
$T_{\mathrm{B}}^{(c)} < T < T_{\mathrm{A}}^{(c)}$	×	metastable	stable
$T_{ m A}^{(c)} < T$	×	×	stable

Table 10: Phases in various temperature ranges for  $N \ge 13$  and their stability.

#### **4.3.10** SU(N) in the $N \gg 1$ limit

The limiting behavior of the various temperatures for  $N \gg 1$  is

$$T_{\rm A}^{(\rm m)} \simeq \frac{T_0}{2}$$
,
$$T_{\rm BA} \simeq T_{\rm AS} \simeq T_0 \frac{N}{4 \ln N}$$
,
$$T_{\rm B}^{(\rm un)} \simeq T_{\rm A}^{(c)} \simeq T_{\rm B}^{(c)} \simeq T_0 \frac{N}{2 \ln N}$$
.
$$(4.18)$$

These have been found using a combination of analytical and numerical methods. We note that even though  $N\gg 1$  we are still in the regime  $N\ll n$ . In this limit, we have  $T_{\rm B}^{({\rm un})}\simeq T_{\rm B}^{(c)}\simeq T_{\rm A}^{(c)}$ , and  $T_{\rm BA}\simeq T_{\rm AS}$ . The last equality implies that the range in which phase A is globally stable shrinks, and B survives as the only stable phase other than the singlet. The single temperature  $T_{\rm BA}\simeq T_{\rm AS}$  marks the transition between B and the singlet, hence we will denote it by  $T_{\rm BS}$ . The transition table simplifies as below. A

Temperature/irrep	В	A	•
$T < T_{ m A}^{( m m)}$	stable	unstable	unstable
$T_{A}^{(m)} < T < T_0$	stable	metastable	unstable
$T_0 < T < T_{\mathrm{BS}}$	stable	metastable	metastable
$T_{\rm BS} < T < T_{\rm A}^{(c)}$	metastable	metastable	stable
$T_{\rm A}^{(c)} < T$	×	×	stable

Table 11: Phases in various temperature ranges for  $N \gg 1$  and their stability.

smaller table 12 is the analog of table 5 for  $N \gg 1$ .

Temperature	$T < T_{\rm BS}$	$T_{\rm BS} < T$
irrep	В	•

Table 12: Stable phases in the various temperature ranges for  $N \gg 1$ .

The evolution of the various critical temperatures  $T_{\rm A}^{(\rm m)}$ ,  $T_{\rm BA}$ , etc. as functions of N is plotted in fig. 6 below. As noted, for  $N\gg 1$  there is no intermediate temperature regime in which the solution A is stable.

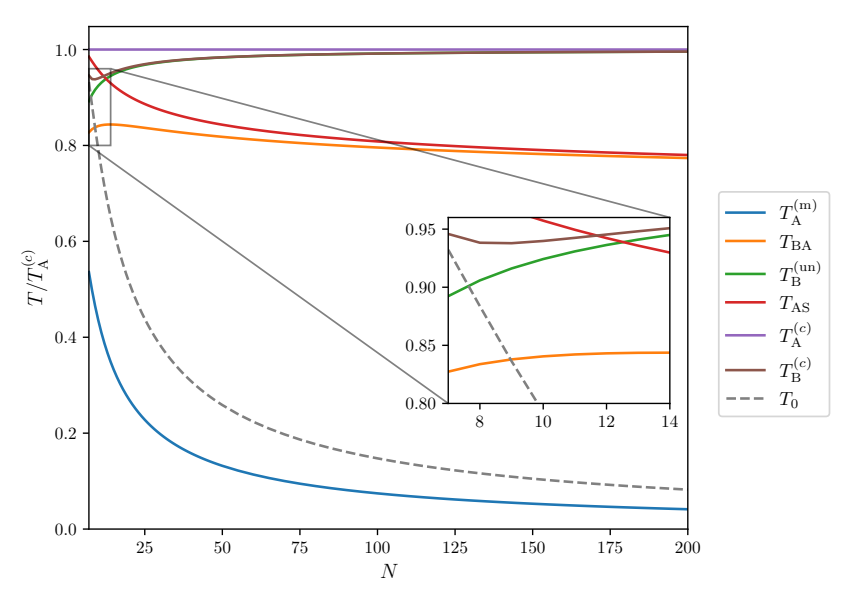


Figure 6: Evolution of the temperatures  $T_{\rm A}^{(\rm m)}$ ,  $T_{\rm BA}$ ,  $T_{\rm B}^{(\rm un)}$ ,  $T_{\rm AS}$ ,  $T_{\rm A}^{(c)}$  and  $T_{\rm B}^{(c)}$  with the group rank N. All temperatures are normalized by  $T_{\rm A}^{(c)}$ . The inset serves to show the crossings between the different temperatures that occur for  $7 \leqslant N \leqslant 13$ . According to (4.18)  $T_{\rm BA}$  and  $T_{\rm AS}$  eventually converge to  $T_{\rm A}^{(c)}/2$ . This becomes visible at extremely large N, due to the slow convergence of  $T_{\rm B}^{(\rm un)}$ ,  $T_{\rm A}^{(c)}$  and  $T_{\rm B}^{(c)}$  to their large N limit, and is not depicted in the figure.

### 4.4 The reducible fundamental-antifundamental representation

To monitor the effects that relatively minor variations of the model have on the results, we consider atoms in the reducible tensor product representation  $\bullet \otimes \Box = \bullet \Box \oplus \mathbb{1}$  which differs form the adjoint by the presence of an additional singlet state per atom. We will see that this affects our results only minimally.

Application of the general formalism to the above representation is straightforward. We note that, in the reducible case, the self-interaction terms  $\sum_{a=1}^{N^2-1} (j_i^a)^2$  that must be eliminated from the mean-field Hamiltonian are not constant Casimirs any more, but their contribution is subleading in n and can be neglected. The analysis results to equilibrium equations and constraints identical to the ones for the adjoint, upon substituting  $\rho^2 \pm 1 \to \rho^2$  and  $N^2 - 1 \to N^2$  in the expressions. This modification leads to a similar phase structure as for the adjoint representation, with some quantitative differences. The values of the critical temperatures  $T_{\rm A}^{(m)}$ ,  $T_{\rm B}^{(m)}$ ,  $T_{\rm BA}$ ,  $T_{\rm AS}$ ,  $T_{\rm A}^{(c)}$  and  $T_{\rm B}^{(c)}$  change slightly, but the tables 1 to 12 remain almost intact. Specifically, tables 2 and 3 hold for N=4 only, table 4 holds for N=5 and 6, table 5 holds for  $N\geqslant 5$ , and all other tables remain unmodified.

Phase transitions are also generally of the same order as in the adjoint case, with the exception of the transition of the A state to the singlet for N = 5, which is no longer of second order at  $T = T_0$ , but becomes first order at  $T_{AS} > T_0$ . Further, the nonanalytic behavior in (4.17) of the adjoint case for N = 5 is now absent.

The case of SU(2) is particularly simple, since its fundamental and antifundamental irreps are equivalent, and thus n reducible representations  $\bullet \otimes \Box$  are equivalent to 2n fundamentals. Equivalently, it corresponds to  $\lambda = 2\lambda_{\text{fund}}$ , and from (2.11) we deduce

$$F(c, \mathbf{x}) = 2 F_{\text{fund}}(2c, \mathbf{x}/2)$$
 (4.19)

Indeed, the equilibrium equation for  $x_1 = -x_2 \equiv x$  and the corresponding free energy coincide with the ones in [20] up to the factors of 2 in (4.19).

### 5 Conclusions

Ferromagnets with atoms in the SU(N) adjoint representation prove to be interesting and intricate physical systems, adding to the already rich array of phenomena

of ferromagnets in the fundamental, symmetric, and antisymmetric representations. The new element is the conjugation invariance of the free energy, which adds a discrete symmetry to the global SU(N) symmetry of the system. Our results reveal that this symmetry can also be spontaneously broken, although in a more restricted temperature range that the magnetization SU(N) symmetry. We expect the spontaneous breaking of conjugation symmetry to be a generic feature of ferromagnets with atoms in an arbitrary self-conjugate representation.

It is interesting that the phase structure we have unveiled depends to a good extent on the rank N of the group, as the large number of phase transition patterns indicates. This dependence appears at nonvanishing temperature and does not seem to have a clear group theoretic origin.

The phase structure of the adjoint ferromagnet shares many of the features of the ferromagnet with atoms in the antisymmetric representation studied in [23], which include the appearance of more than two phases, and regimes in which they coexist as stable and metastable states. The presence of metastable states is physically significant, since their thermally driven transition to a fully stable state takes an exponentially long time. Thus, metastable states are practically stable if left unperturbed, and only external perturbations (impurities, shaking the system etc.) can catalyze their decay.

The symmetry breaking patterns of the adjoint ferromagnet validate the general conjectures put forth in our previous work [23]. One of them was that, if the atom irrep  $\chi$  has r rows, the ferromagnet will have up to r+1 distinct phases corresponding to irreps with  $0,1,\ldots,r$  rows (0 rows corresponding to the singlet). The adjoint can be thought of as a two-row state, with one row and one antirow, and indeed its stable phases are the singlet, one row, one antirow, and the (self-conjugate) one row plus one antirow irreps, in agreement with the conjecture. Further, the critical temperature  $T_0^{(\chi)}$  below which the singlet becomes unstable has the general conjectured form (C.1) in terms of group theoretical quantities. Proving the above conjectures for a general atom representation is an interesting open question.

Physical applications of our adjoint ferromagnet can vary, but they fall within the general category of couplings that are not fully invariant under atom state rotations (interactions are not of purely exchange type). Specific situations where the adjoint is relevant will involve systems with conjugation invariance, and their experimental realization is of substantial physical interest.

The work in this paper extends the results of [23] in one of several possible directions, namely to a different higher atom irrep. Coupling the atoms to magnetic fields, which can be studied with the existing formalism, would be useful for probing the response of the states to external fields. Other generalizations suggested in [20, 23], e.g., including three- and higher-atom interactions for the adjoint, as was done for the fundamental in [24], or inclusion of interaction terms along the Cartan generators breaking the SU(N) invariance, remain open to investigation. The study of the adjoint model in the double scaling large-N limit  $N \sim \sqrt{n}$  studied in [21,22] for fundamental atoms is also interesting. We expect that the large-N limiting behavior in the scaling  $N \sim \sqrt{n}$  will lead to transitions into "disjoint" phases at large temperature. Further, the relevance of our results to nonabelian topological phases in one dimension [27–30] and the persistence of such phases in higher dimensions are interesting questions for future investigation.

In a different direction, our results for SU(N) ferromagnets bear a tantalizing resemblance to those of N-state Potts spin models on a complete graph, recently studied in the context of models for collective communication and competition in social systems [31]. The relevance of our adjoint and other higher irrep ferromagnets to social systems is a fascinating topic that merits exploration.

Finally, extending our ferromagnetic model to other classical groups, supersymmetric groups with fermionic dimensions, or "quantum" *q*-groups are interesting possibilities and offer avenues for further research.

### Acknowledgements

A.P. would like to thank Sergei Nechaev for interesting discussions. A.P.'s research was supported by the National Science Foundation under grants NSF-PHY-2112729 and NFS-PHY-2112479, and by PSC-CUNY grants 67100-00 55 and 6D136-00 05.

# A On conjugate representations

Elaborating on the notion of conjugation, consider a YT with  $p_i$  rows of length  $\ell_i$ , i = 1, 2, ..., N - 1. The conjugate YT is obtained by subtracting the original YT from the  $\ell_1 \times N$  rectangle framing it and rotating the remainder by  $180^o$  (this can be equiv-

alently thought of as turning all rows into antirows). As an example, the conjugate of the YT with  $p_1$  rows of length  $\ell_1$  and  $p_2$  rows of length  $\ell_2 < \ell_1$  (equivalently,  $p_1$  rows of length  $\ell_1 - \ell_2$  and  $N - p_1 - p_2$  antirows of length  $\ell_2$ ) has  $N - p_1 - p_2$  rows of length  $\ell_1$  and  $\ell_2$  rows of length  $\ell_1 - \ell_2$ . If  $N - p_1 - p_2 = p_1$  (that is,  $2p_1 + p_2 = N$ ) and  $\ell_1 - \ell_2 = \ell_2$  (that is,  $2\ell_2 = \ell_1$ ), then the YT maps to itself under conjugation and is self-conjugate. This is possible only if  $\ell_1$  is even. However, in our case this is immaterial since row lengths scale with the number of atoms  $n \gg 1$ . Note that the number of boxes in a self-dual YT of the above type is  $N\ell_1/2$  and hence independent of  $p_1$ .

### B More generic, unstable solutions

Besides the solutions A and B, one may wonder if there are other stable solutions. It turns out that there are none. Any modification of these solutions results to instability for all temperatures.

The simplest such example is solutions with  $p_1 = 1$  and  $p_2 = N - 2$  with general values of  $\alpha_i$ . We present all different solutions for comparison, including A, B, the singlet, as well as these new solutions, in fig. 7 for N = 5 and N = 7. The new solutions start as type A for  $T = T_A^{(m)}$  and then, as the temperature increases, they become an intermediate configuration between type A and type B. Finally, they become a type B configuration at  $T = T_B^{(un)}$ . We call these solutions AB and, schematically, they correspond to the following YT

$$AB:$$
 or  $\bullet \bullet \bullet \bullet$ . (B.1)

This may be thought of as resulting from the solution (3.22) by adding dots on the left YT and removing dots from the right YT.

Other solutions, also unstable, can be found for values of  $(p_1, p_2) \neq (1, N-2)$ . These solutions violate the self-conjugation symmetry. For the simplest case with  $(p_1, p_2) = (1, N-3)$  and all three  $\alpha_i$  different, the stability matrix  $T \mathbb{1} - c\Lambda$  has negative eigenvalues for all temperatures. We plotted these eigenvalues, in the indicative case N=5, as a function of the temperature in fig. 8. Such solutions corresponds to YTs of the general form (3.15). In particular, for the case with  $(p_1, p_2) = (1, N-3)$  they assume the form

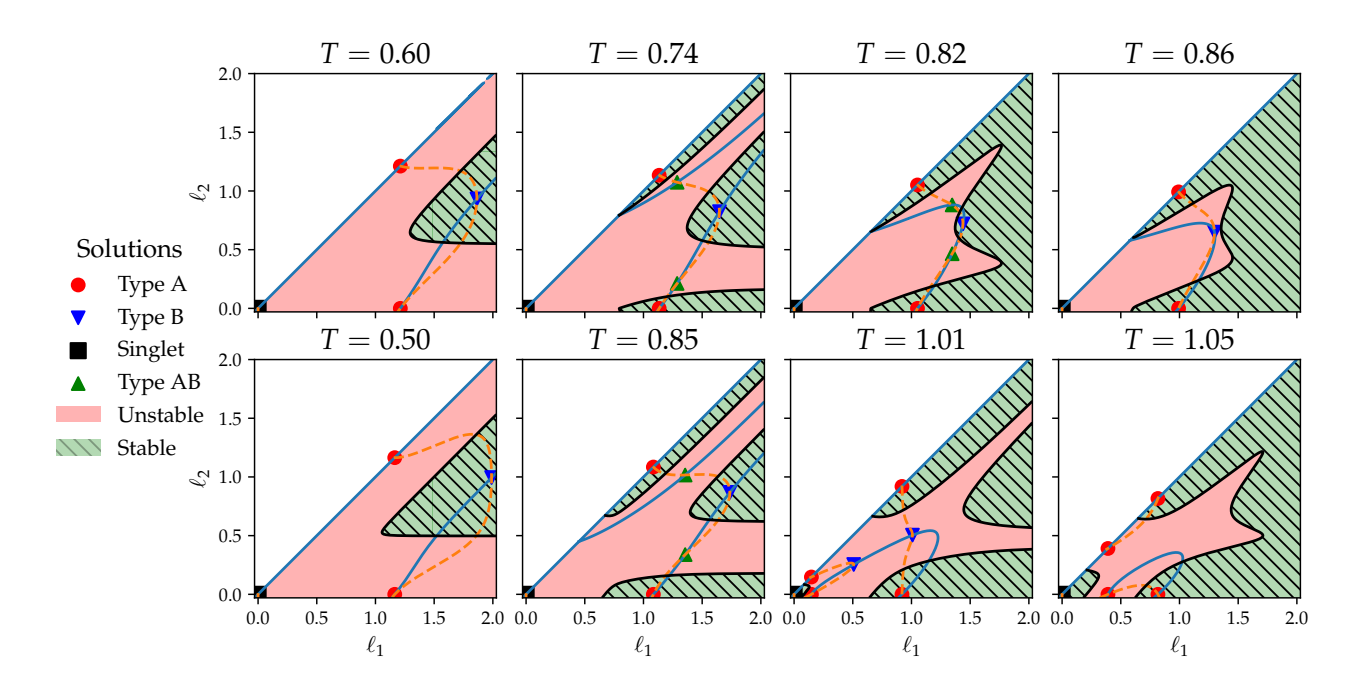


Figure 7: Stable and unstable YT configurations, for N=5 (top four subplots) and N=7 (bottom four subplots) and various temperatures, as denoted by the plots' titles. Temperatures are in units of  $T_0$  and the lengths of YTs are in units of  $T_0$ . All plots correspond to  $T_0 = 1$  and  $T_0 = 1$  are in units of  $T_0 = 1$  and  $T_0 = 1$  are in units of  $T_0 = 1$  and  $T_0 = 1$ 

For both N=5 and N=7, the singlet  $\ell_1 = \ell_2 = 0$  is stable only for  $T > T_0$ .

For N=5, the first plot corresponds to temperature  $T < T_{\rm A}^{\rm (m)}$  where only the type B solution is stable. The second and third plots correspond to temperatures  $T_{\rm A}^{\rm (m)} < T < T_{\rm B}^{\rm (un)}$ , where both type A and B solutions are locally stable. In this temperature range, a pair of solutions of type AB emerge. These solutions are always unstable, and they represent YT configurations intermediate between types A and B, as in (B.1), becoming type A as  $T \to T_{\rm A}^{\rm (un)}$  and type B as  $T \to T_{\rm B}^{\rm (un)}$ . The lower (upper) AB solution corresponds to the left (right) YT in (B.1). Finally, the fourth plot corresponds to a temperature  $T_{\rm B}^{\rm (un)} < T < T_{\rm 0}$ , where the type A solution is stable but the type B is not.

For N=7, the first plot corresponds to temperature  $T < T_{\rm A}^{\rm (m)}$  where only the type B solution is stable. The second plot corresponds to temperatures  $T_{\rm A}^{\rm (m)} < T < T_{\rm B}^{\rm (un)}$ , where both type A and B solutions are stable. In this range a pair of solutions of type AB emerge, which are always unstable. The third plot corresponds to temperature  $T_{\rm B}^{\rm (un)} < T_0 < T < T_{\rm B}^{(c)}$ , where the type A solution and singlet are (meta)stable, but the type B one is not. Lastly, the fourth plot corresponds to temperatures  $T_{\rm B}^{\rm (c)} < T < T_{\rm A}^{\rm (c)}$ , where only the singlet and type A solutions exist and are (meta)stable, and some of the type A solutions are unstable.

Similar plots to fig. 8 can be produced for higher values of N, but we will not present them here.

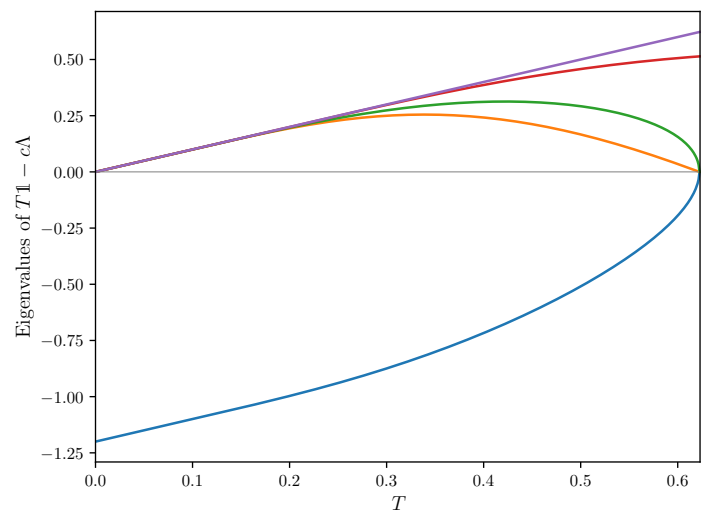


Figure 8: Eigenvalues of a generic solution, for N = 5,  $p_1 = 1$  and  $p_2 = 2$ , as a function of temperature, which is in units of  $T_0$ . This solution exists for temperatures  $T \lesssim 0.622$ . One eigenvalue is always negative and hence the solution is unstable.

# C Some group theory results

It is interesting that the parametrization of the ferromagnetic coupling constant c in (3.10) in terms of the critical temperature  $T_0$  below which the singlet becomes unstable can be written in the form

$$c = \frac{T_0}{2} \frac{\dim G}{C_{\chi}^{(2)}} \,, \tag{C.1}$$

where dim G is the dimension of the group (here, SU(N)) and  $C_{\chi}^{(2)}$  is the eigenvalue of the corresponding quadratic Casimir operator. This expression was conjectured in [23] and was shown to work for the fundamental, symmetric, and antisymmetric irreps. Here we fill some details and show that (C.1) also holds for the adjoint representation. The quadratic Casimir operator is given by [25]

$$C_2(\mathbf{k}) = \frac{1}{2} \sum_{i=1}^{N} \left( k_i - \frac{k}{N} \right)^2 - \frac{N(N^2 - 1)}{24} , \quad k = \sum_{i=1}^{N} k_i .$$
 (C.2)

The corresponding YT has N-1 rows with length given by

$$\ell_i = k_i - k_N + i - N$$
,  $i = 1, 2, ..., N - 1$ . (C.3)

The singlet corresponds to  $k_i = N - i$ , i = 1, ..., N. For the fundamental representation we increase  $k_1$  by one, leaving the other  $k_i$ 's as they are. For the symmetric

representation we increase  $k_1$  by two, whereas for the antisymmetric representation we increase  $k_1$  as well as  $k_2$  by one. For the adjoint representation we increase  $k_1$  by two and  $k_i$ , for i = 2, 3, ..., N-1, by one. Using the above, we find for the irreps we consider

$$C_{\text{fund}}^{(2)} = \frac{N^2 - 1}{2N}, \qquad C_{\text{sym}}^{(2)} = \frac{(N - 1)(N + 2)}{N},$$

$$C_{\text{ant}}^{(2)} = \frac{(N - 2)(N + 1)}{N}, \qquad C_{\text{adj}}^{(2)} = N.$$
(C.4)

The expressions for these Casimirs are, of course, well known, but we wanted to fix the normalization and make contact with the **k** representation. Clearly, for G = SU(N) we have dim  $G = N^2 - 1$  and (C.1) reduces to (3.10).

# References

- [1] R.A. Duine and A.H. MacDonald, *Itinerant Ferromagnetism in an Ultracold Atom Fermi Gas*, Phys. Rev. Lett. **95** (2005) 230403
- [2] M.A. Cazalilla, A.F. Ho and M. Ueda, *Ultracold gases of ytterbium: ferromagnetism and Mott states in an SU*(6) *Fermi system*, New J. Phys. **11** (2009) 103033.
- [3] A.V. Gorshkov et al., Two-orbital SU(N) magnetism with ultracold alkaline-earth atoms, Nature Physics 6 (2010) 289-295.
- [4] X. Zhang et al., Spectroscopic observation of SU(N)-symmetric interactions in Sr orbital magnetism, Science Vol 345, Issue 6203 (2014) 1467.
- [5] M. A. Cazalilla and A.M. Rey, *Ultracold Fermi gases with emergent SU(N) symmetry*, 2014 Rep. Prog. Phys. 77 124401.
- [6] S. Capponi, P. Lecheminant, and K. Totsuka, *Phases of one-dimensional SU(N) cold atomic Fermi gases From molecular Luttinger liquids to topological phases*, Ann. Phys. **367** (2016) 50-95.
- [7] B. Mukherjee, J.M. Hutson and K. R. A. Hazzard, SU(N) magnetism with ultracold molecules, New J. Phys. **27** 013013, 2404.15957 [cond-mat.quant-gas].
- [8] I. Affleck, Large-n Limit of SU(n) Quantum "Spin" Chains, Phys. Rev. Lett. **54** (1985) 966.

- [9] A.P. Polychronakos, *Exact Spectrum of SU(n) Spin Chain with Inverse-Square Exchange*, Nucl. Phys. **B419** (1994) 553-566, hep-th/9310095.
- [10] H. Katsura and A. Tanaka, *Nagaoka states in the SU*(n) *Hubbard model*, Phys. Rev. **A87**, 013617 (2013).
- [11] E. Bobrow, K. Stubis and Y. Li, Exact results on itinerant ferromagnetism and the 15-puzzle problem, Phys. Rev. **B98**, 180101(R) (2018).
- [12] C. Romen and A.M. Läuchli, *Structure of spin correlations in high-temperature* SU(N) *quantum magnets*, Phys. Rev. Research **2** (2020) 043009.
- [13] D. Yamamoto, C. Suzuki, G. Marmorini, S. Okazaki and N. Furukawa, *Quantum and Thermal Phase Transitions of the Triangular SU*(3) *Heisenberg Model under Magnetic Fields*, Phys. Rev. Lett. **125**, 057204 (2020).
- [14] K. Tamura and H. Katsura, Ferromagnetism in d-Dimensional SU(n) Hubbard Models with Nearly Flat Bands, Journal of Stat. Phys. volume **182**, 16 (2021).
- [15] K. Totsuka, Ferromagnetism in the SU(N) Kondo lattice model: SU(N) double exchange and supersymmetry Phys. Rev. **A107**, 033317 (2023).
- [16] K. Tamura, H. Katsura *Flat-band ferromagnetism in the SU(N) Hubbard and Kondo lattice models*, 2303.15820 [cond-mat].
- [17] D. Yamamoto et al., Quantum and Thermal Phase Transitions of the Triangular SU(3) Heisenberg Model under Magnetic Fields,
  Phys. Rev. Lett. **125** (2020) 057204, 2004.03250 [cond-mat].
- [18] Y. Miyazaki et al., Linear Flavor-Wave Analysis of SU(4)-Symmetric Tetramer Model with Population Imbalance,
  J. Phys. Soc. Jpn. 91 (2022) 073702, 2205.11155 [cond-mat].
- [19] H. Motegi. G. Marmorini, N. Furukawa, D. Yamamoto, Thermal Ising transition in two-dimensional SU(3) Fermi lattice gases with population imbalance, Phys. Rev. Research 5 L022056, 2209.05919 [cond-mat].
- [20] A.P. Polychronakos and K. Sfetsos, *Ferromagnetic phase transitions in SU(N)*, Nucl. Phys. **B996** (2023), 116353, 2306.01051 [hep-th].

- [21] A.P. Polychronakos and K. Sfetsos, *Phase transitions in the decomposition of* SU(N) *representations*, Nucl. Phys. **B999** (2024), 116434, 2310.16887 [hep-th].
- [22] A.P. Polychronakos and K. Sfetsos, *Triple critical point and emerging temperature scales in SU(N) ferromagnetism at large N*,
  Nucl. Phys. **B1009** (2024), 116748, 2408.08357[hep-th].
- [23] A. P. Polychronakos and K. Sfetsos, Ferromagnets from higher SU(N) representations, Nucl. Phys. **B1014** (2025) 116880, arXiv:2501.11681 [hep-th].
- [24] A.P. Polychronakos and K. Sfetsos, *Nonabelian ferromagnets with three-body interactions*, Nucl. Phys. **B1018** (2025) 117094 arXiv:2506.19916 [hep-th].
- [25] A.P. Polychronakos and K. Sfetsos, *Composing arbitrarily many SU*(N) *fundamentals*, Nucl. Phys. **B994** (2023) 116314, arXiv:2305.19345 [hep-th].
- [26] A.P. Polychronakos and K. Sfetsos, *Composition of many spins, random walks and statistics*, Nucl. Phys. **B913** (2016), 664-693, 1609.04702 [hep-th].
- [27] K. Totsuka, P. Lecheminant, and S. Capponi, *Semiclassical approach to competing orders in a two-leg spin ladder with ring exchange*, Phys. Rev. **B86** (2012) 014435.
- [28] A. Roy and T. Quella *Chiral Haldane phases of* SU(N) *quantum spin chains,* Phys. Rev. **B 97** (2018) 155148.
- [29] S. Capponi, P. Fromholz, P. Lecheminant and K. Totsuka, Symmetry-protected topological phases in a two-leg SU(N) spin ladder with unequal spins, Phys. Rev. B101 (2020) 195121.
- [30] K. Remund, R. Pohle, Y. Akagi, J. Romhanyi and N. Shannon, *Semi-classical simulation of spin-1 magnets*, Phys. Rev. Res. 4 (2022) 033106.
- [31] P. Akarapipattana, S. Nechaev and B. Slavov, *Collective communication in a transparent world: Phase transitions in a many-body Potts model and social-quantum duality*, arXiv:2508.20267 [hep-th].